34th Annual International Conference of the IEEE EMBS
San Diego, California USA, 28 August - 1 September, 2012

Carotid Far Wall Characterization using LBP, Laws ' Texture Energy and Wall Variability: A Novel Class of Atheromatic Systems

U Rajendra Acharya, Vinitha Sree S*, Muthu Rama Krishnan M, Luca Saba, Filippo Molinari, Shoaib Shafique, Andrew Nicolaides, Jasjit S Suri, Fellow AIMBE

***Abstract*— In this work, we present a Computer Aided Diagnostic (CAD) technique (a class of Atheromatic systems) that classifies the automatically segmented carotid far wall Intima-Media Thickness (IMT) regions along the common carotid artery into symptomatic and asymptomatic classes. We extracted texture features based on Local Binary Patterns (LBP) and Law's Texture Energy (LTE) and used the significant features to train and test the Support Vector Machine classifier. We developed the classifiers using three-fold stratified cross validation data resampling technique on 342 IMT wall regions. An accuracy of 89.5% was registered. Thus, the proposed technique is accurate, robust, non-invasive, fast, objective, and cost-effective, and hence, will add more value to the existing carotid plaque diagnostics protocol.**

***Index Terms*— Atherosclerosis, Symptomatic, Asymptomatic, Carotid Far Wall, Local Binary Patterns, Laws' Texture Energy, Wall Variability, Classifiers.**

I. Introduction

Carotid atherosclerosis results in carotid stenosis which has been found to cause ischemic strokes. Stroke risk can be reduced by removing the plaque by Carotid Endarterectomy (CEA)) or by using Carotid Artery Stenting (CAS). However, both these procedures carry risks [1], and hence, it is advisable to offer them to only symptomatic patients who carry more risk of rupture that result in dangerous embolization [2]. Currently, selection of patients to be considered for endarterectomy is based on the previous history of occurrence of clinical symptoms such as stroke, Transient Ischaemic Attack (TIA), Amaurosis Fugax (AF) and the degree of stenosis caused by the plaque [3]. However, it has been observed that plaques with relatively low stenosis degree may produce symptoms [4] and the majority of asymptomatic patients with highly stenotic plaques may remain asymptomatic [5]. Therefore, there is a need to identify more features that characterize and classify plaques belonging to symptomatic and asymptomatic groups. In this work, we have proposed a novel data mining framework that extracts texture features such as Local Binary Pattern (LBP) and Laws' Texture Energy (LTE) from carotid far walls referred to as the Intima-Media Thickness (IMT) regions in carotid ultrasound images. Several studies have indicated that progressive atherosclerotic lesions begin with a pathological thickening of the intimal wall region [6,7]. Therefore, to detect symptomatic cases when the plaque is at its very early stage, we have attempted to extract the IMT wall region for feature extraction.

Fig. 1 depicts the general block diagram of the proposed Atheromatic technique. In Fig. 1, all the blocks outside the shaded rectangular box represent the flow of the off-line training procedure, and the blocks inside the shaded box indicate the on-line real-time system. In the off-line training system, first we pre-process the training images, and then automatically segment the far wall IMT Region of Interest (ROI) along with its IMT variability (IMTV). The texture features are then extracted from this ROI. Significant features are selected using the Student's *t-test*. The significant features and the ground truth (original classification by the physicians as to whether the given ROI is symptomatic or asymptomatic) are used to train the classifier in order to obtain the training parameters. These features and the training parameters are used by the classifier to determine the class of the plaque, and subsequently, the output classification labels are used to determine the performance measures like accuracy, sensitivity, specificity, and Positive Predictive Value (PPV).

II. Materials and Methods

A. Ultrasound Image Acquisition and Pre-processing

We procured two datasets, one from Hong Kong, and one from Italy. In the Hong Kong dataset, all the patients had no symptoms prior to the ultrasound examination, and hence, the acquired images were considered asymptomatic. The 50 studied subjects were part of the cohort of a longitudinal study conducted at the Department of Imaging and Interventional Radiology, The Chinese University of Hong

Manuscript received January 30, 2012.

U. Rajendra Acharya and Muthu Rama Krishnan M are with the Department of Electronics and Computer Engineering, Ngee Ann Polytechnic, Singapore

Vinitha Sree is with Global Biomedical Technologies Inc., CA, USA (email: vinitha.sree@gmail.com)

Filippo Molinari is with Biolab, Department of Electronics and Telecommunications, Politecnico di Torino, Torino, Italy.

Luca Saba is with the Department of Radiology, Azienda Ospedaliero Universitaria di Cagliari, Cagliari, Italy

Andrew Nicolaides is with the Vascular Screening and Diagnostic Centre, London, and Department of Biological Sciences, University of Cyprus, Nicosia, Cyprus

Shoaib Shafique, MD, is with CorVas, West Lafayette, Indiana, USA.

Jasjit S. Suri, Fellow AIMBE, is a CTO with AtheroPoint LLC, CA, USA and Global Biomedical Technologies, CA, USA and is also affiliated with Biomedical Engineering Department, Idaho State University, ID, USA (jsuri@comcast.net).

Kong. The carotid arteries were examined using a 13-5 MHz linear transducer of Sonoline Antares ultrasound scanner. Both distal common carotid arteries of each subject were imaged from three multiple views using three different approaches: anterior, anterolateral and posterolateral with simultaneous ECG gating. Thus, six images were acquired from each patient, three from the left carotid artery and three from the right to create a database of 300 asymptomatic carotid wall images.

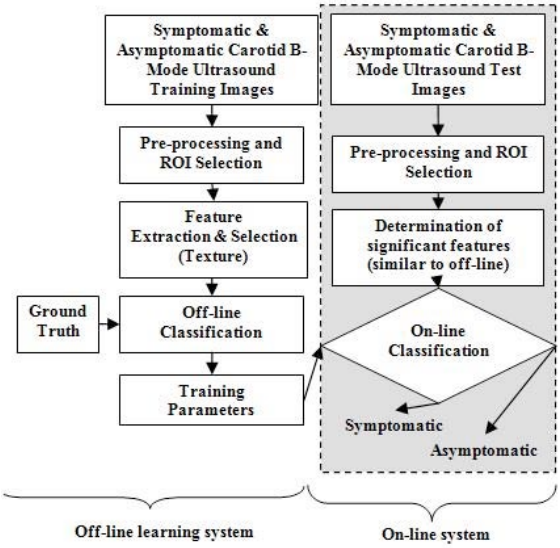

Fig. 1. Block diagram of the proposed system; The blocks outside the dotted shaded rectangular box represent the flow of off-line training system, and the blocks within the dotted box represent the on-line real-time system

To get the Italy dataset, a total of 21 in-patients were retrospectively studied using Color Duplex Ultrasound Scanning (CDUS) at the Department of Radiology, A.O.U. di Cagliari, Italy. CDUS was done using Esaote MyLab™ 70 modality with a 10 MHz linear-array transducer. The patient's head was tilted to image the carotid artery that was just proximal to the bulb placed horizontally across the screen [8]. Among the 21 patients, 11 were symptomatic and 10 were asymptomatic. Two images, one from the left carotid and one from the right carotid, were obtained from each patient. Therefore, from the 10 asymptomatic cases, we obtained 20 asymptomatic images. In the 11 symptomatic cases, we considered the carotid ipsilateral to the symptom as symptomatic i.e. if the stroke was on the right side, the right carotid was considered symptomatic and the left asymptomatic. Thus, from these 11 cases, we obtained 11 symptomatic and 11 asymptomatic images. Therefore, there were 20+11=31 asymptomatic carotids and 11 symptomatic carotids. Overall, from both the wall datasets, we had 331 asymptomatic and 11 symptomatic images.

B. ROI Segmentation

In the ultrasound image, we automatically segmented the region between the Lumen-Intima (LI) and Media-Adventitia (MA) interfaces of the Common Carotid Artery (CCA) and called it the IMT region. Since manual measurement of IMT is time consuming, subjective, and tedious, several CAD tools (in the class of AtheroEdge™ class of systems) that are either fully or partially automated have been developed [9]. In these algorithms, IMT is calculated automatically using two key steps: (1) Recognition of the CCA, and tracing of the Near Adventitia (AD_N) and Far Adventitia (AD_F) layers. (2) Determination of the LI and MA borders, and calculation of IMT and IMT wall region. Under the class of AtheroEdge™, Global Biomedical Technologies Inc. has developed different patented paradigms of automatic IMT measurement and far wall segmentation systems. In this work, we used CAMES (Completely Automated Multi-resolution Edge Snapper) algorithm which is a fully automated algorithm for CCA recognition and subsequent LIMA segmentation [10]. This algorithm utilizes the morphological properties of the CCA to determine the IMT. Fig. 2 (WA1) and (WS1) show the symptomatic and asymptomatic wall images. Fig. 2 (WRA1) and (WRS1) show the respective far wall regions.

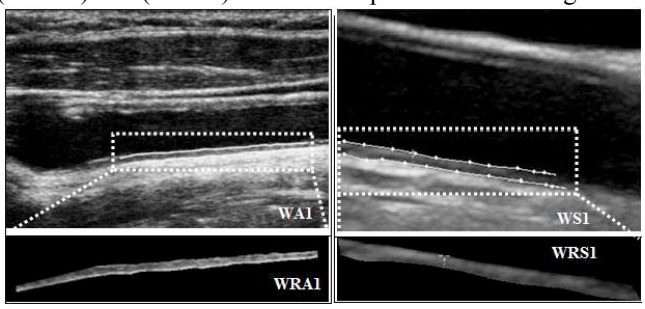

Fig. 2. Carotid Asymptomatic Wall Image (WA1); Symptomatic Wall Image (WS1). Corresponding Extracted Wall Regions WRA1 and WRS1

C. Feature Extraction

In the IMT wall region, we determined features such as LBP and LTE, and also calculated the wall variability by studying the deviations of the mean IMT along the carotid far wall.

Local Binary Pattern (LBP): The LBP feature vector is determined as follows [11]: A circular neighborhood is considered around a pixel. P points are chosen on the circumference of the circle with radius R such that they are all equidistant from the center pixel. Let g_c be the gray value of the centre pixel and g_p, $p=0,\ldots, P-1$, corresponds to the gray values of the P points. These P points are converted into a circular bit-stream of 0's and 1's according to whether the gray value of the pixel is less than or greater than the gray value of the center pixel. Let U be the number of spatial bitwise 0/1 transitions. In this work, a rotation invariant measure called $LBP_{P,R}$ was calculated. Only patterns with $U \leq 2$ were assigned the LBP code as follows:

$$LBP_{P,R}(x) = \begin{cases} \sum_{p=0}^{P-1} s(g_p - g_c) & if \quad U(x) \leq 2 \\ P+1 & otherwise \end{cases} \tag{1}$$

where, $s(x) = \begin{cases} 1, x \geq 0 \\ 0, x < 0 \end{cases}$

Multi-scale analysis using LBP is done by choosing circles with various radii around the centre pixels and

constructing separate LBP image for each scale. In our work, energy and entropy of the LBP image, constructed over different scales (R=1, 2, and 3 with the corresponding pixel count P being 8, 16, and 24, respectively) were used as feature descriptors.

Laws Texture Energy (LTE): Laws used masks of appropriate sizes for discriminating between different kinds of texture [12]. In this work, all the masks were derived from one-dimensional (1D) vectors: L3: [1, 2, 1], E3: [−1, 0, 1], and S3: [−1, 2, − 1] that describe the following features: level, edge, and spot, respectively. By convoluting any vertical 1D vector with a horizontal one, nine 2D masks of size 3 × 3, namely, *L3L3, L3E3, L3S3, E3E3, E3L3, E3S3, S3S3, S3L3, S3E3* were generated. Among these nine masks, we used eight zero-sum masks numbered 1 to 8. To extract texture information, the image was first convoluted with each 2D mask to obtain the corresponding texture image (eg. TI_{E3E3}). According to Laws, all the 2D masks, except *L3L3* had zero mean. Hence, texture image TI_{L3L3} was used to normalize the contrast of all other texture images *TI (i,j)*. The outputs (*TI*) were passed to "texture energy measurements" filters. These consisted of a moving non-linear window average of absolute values. Thus, in this work, the image under inspection was filtered using these eight masks, and their energies were computed and used as feature descriptors [13].

***Wall IMT Variability as a Feature*:** In order to calculate the distance between LI and MA borders, which represents the IMT, the Polyline Distance Measure (PDM) was used in this work. PDM measures the distance of each vertex of one boundary to the segments of the second boundary. A recent study [14] shows that the wall variability may be associated with atherosclerosis. In this work, we have quantified wall variability by a novel feature called the $IMTV_{poly}$ which is the standard deviation of the IMT.

D. K-Nearest Neighbor (KNN)

K-Nearest Neighbor (KNN) classifier is a simple classifier in which a feature vector is assigned the class that is the most common among its K nearest neighbors [15]. K is typically a small positive integer.

III. Results

A. Selected Features

We used t-test [16] to verify if the features are significant enough to be able to accurately discriminate the symptomatic and asymptomatic classes. Table 1 presents the Mean ± Standard Deviation (SD) of the significant features. A p-value of less than 0.0001 indicates that the features are significant. $LBP_{324}Ene$ has registered a significantly higher value for the asymptomatic images compared to symptomatic images. It is also evident that LTE_2Ene is more powerful than LTE_8Ene as the difference in the LTE_2Ene values for both the classes is higher than that for LTE_8Ene. This is because the mask 2 used to calculate LTE_2Ene captures more information about the level, edges, and spots in the image than those captured by the mask 8 used to obtain LTE_8Ene. The $IMTV_{poly}$ feature has a higher value for the symptomatic images than for the asymptomatic images. This indicates that the wall variability is higher in the case of symptomatic images.

TABLE I
SIGNIFICANT FEATURES THAT HAD A P-VALUE < 0.0001 AND THEIR RANGES (MEAN±SD) FOR SYMPTOMATIC AND ASYMPTOMATIC CLASSES

Feature	Asymptomatic	Symptomatic	*p*-value
LBP(R=3,P=24)Energy ($LBP_{324}Ene$)	0.3096±0.1272	0.9137 ±0.1957	0.0000
Laws Texture Energy 2 (LTE_2Ene)	4.8117e+006 ±3.7818e+006	3.1159e+007 ±1.6741e+007	0.0000
Laws Texture Energy 8 (LTE_8Ene)	2.3464e+006 ±2.3664e+006	1.9635e+007 ±1.3902e+007	0.0000
$IMTV_{poly}$	0.484 ±0.191	0.104± 8.298E-02	0.0000

B. Atheromatic Classification Results

Three-fold stratified cross validation method was used to evaluate these classifiers. In this method, the dataset was split into three parts, each part containing the same proportion of images from both classes. In the first fold, two parts were used for training and the third part was used for testing and for calculation of the performance measures. This protocol was repeated two more times with a different part as the test set. The averages of the performance measures (sensitivity, specificity, PPV, and accuracy) obtained during the testing phase of each fold are reported as the final performance measures. On excluding $IMTV_{poly}$, the accuracy registered by the KNN classifier was only 88.6%. The sensitivity, specificity, and PPV were 89.6%, 55.6%, and 98.7% respectively. Once $IMTV_{poly}$ was included, an improved accuracy of 89.5% was registered. The sensitivity, specificity, and PPV were also higher: 89.6%, 88.9%, and 99.7%, respectively.

IV. Discussion

A study of the literature reveals that there are only a few CAD algorithms for plaque classification. A comprehensive review of most of these studies can be found in [17]. All these studies [18-20] are based on plaque classification. In this work, however, our objective was to developed an Atheromatic system - a data mining framework to detect symptomatic cases when the plaque is at its very early stage. Therefore, we extracted texture features from the automatically segmented IMT wall region and used them for classification. In the evaluated dataset, the number of symptomatic images was considerably less than the number of asymptomatic images. *i.e.,* only 3% of the dataset had symptomatic images. However, a high accuracy of nearly 90% was achieved in classifying this dataset. Such a classification is only possible because of the highly discriminating features including the novel wall variability feature $IMTV_{poly}$. The powerful capability of the $IMTV_{poly}$ feature was also demonstrated by the significant increase in

the specificity obtained when this feature was included for classification. The use of a reasonably large dataset and the stratified cross validation technique ensure that the training parameters are generalized to accurately and reliably classify new images. The technique is low cost for the following reasons: (a) use of a small feature set, which reduces computational cost, (b) incorporation of the algorithms and indices into existing clinical analysis software at no cost, and (c) use of commonly available ultrasound images. Moreover, all the steps, namely the carotid artery segmentation, measurement of the LI and MA borders, measurement of IMT and IMT wall variability ($IMTV_{poly}$), grayscale feature extraction and selection, and classification, are completely automated, and hence, the technique is highly objective.

We believe that there is a scope of improving the efficiency by adding more features which can represent atherosclerotic deposits in wall region. We also plan to evaluate the proposed techniques using a larger dataset. A drawback of the ground truth determination based on presence or absence of symptoms is that some of the asymptomatic plaques might have been wrongly labelled as symptomatic when the symptoms might have occurred due to plaque in heart and not in the carotid artery. Also, patients who do not recollect their history of symptoms may be classified as asymptomatic. To alleviate this problem, in future, we intend to determine the ground truth from pathological studies on the plaque instead of from the clinical report on the patient's symptoms.

V. CONCLUSION

In this work, we have presented a CAD tool (called Atheromatic system) for carotid far wall region characterization and classification into symptomatic and asymptomatic classes in an attempt to detect early changes in the wall region. Using three significant texture features based on Local Binary Patterns (LBP) and Law's Texture Energy (LTE) paradigms and the IMT wall variability feature in a KNN classifier, we obtained a high accuracy of 89.5%. The system is completely automated, cost-effective, and can be used as an adjunct technique for real-time carotid wall region analysis. In the future, we intend to evaluate the technique using large datasets collected in multi-centre trials and improve the accuracy by using other features.

REFERENCES

[1] T. G. Brott, R. W. Hobson, G. Howard, G. S. Roubin, W. M. Clark, W. Brooks, A. Mackey, M. D. Hill, P. P. Leimgruber, A. J. Sheffet, V. J. Howard, W. S. Moore, J. H. Voeks, L. N. Hopkins, D. E. Cutlip, D. J. Cohen, J. J. Popma, R. D. Ferguson, S. N. Cohen, J. L. Blackshear, F L. Silver, J. P. Mohr, B. K. Lal, and J. F. Meschia, "Stenting versus endarterectomy for treatment of carotid-artery stenosis," *N. Engl. J. Med*., vol. 363, no. 1, pp. 11-23, Jul. 2010.

[2] S. Carr, A. Farb, W. H. Pearce, R. Virmani, and J. S. Yao, "Atherosclerotic plaque rupture in symptomatic carotid artery stenosis," *J. Vasc. Surg.,* vol. 23, no. 5, pp. 755-765, May 1996.

[3] A. N. Nicolaides, S. K. Kakkos, M. Griffin, M. Sabetai, S. Dhanjil, T. Tegos, D. J. Thomas, A. Giannoukas, G. Geroulakos, N. Georgiou, S. Francis, E. Ioannidou, and C. J. Doré, "Asymptomatic Carotid Stenosis and Risk of Stroke (ACSRS) Study Group. Severity of asymptomatic carotid stenosis and risk of ipsilateral hemispheric ischaemic events: results from the ACSRS study," *Eur. J. Vasc. Endovasc. Surg.,* vol. 30, pp. 275-284, 2005.

[4] J. F. Polak, L. Shemanski, D. H. O'Leary, D. Lefkowitz, T. R. Price, P. J. Savage, W. E. Brant, and C. Reid, "Hypoechoic plaque at US of the carotid artery: an independent risk factor for incident stroke in adults aged 65 years or older. Cardiovascular Health Study," *Radiology*, vol. 208, no. 3, pp. 649-654, Sep. 1998.

[5] D. Inzitari, M. Eliasziw, P. Gates, B. L. Sharpe, R. K. Chan, H. E. Meldrum, and H. J. Barnett, "The causes and risk of stroke in patients with asymptomatic internal-carotid-artery stenosis. North American Symptomatic Carotid Endarterectomy Trial Collaborators," *N. Engl. J. Med.*, vol. 342, no. 23, pp.1693-700, Jun. 2000.

[6] R. Virmani, F. D. Kolodgie, A. P. Burke, A. Farb, and S. M. Schwartz "Lessons from sudden coronary death: a comprehensive morphological classification scheme for atherosclerotic lesions," *Arterioscler. Thromb. Vasc. Biol.*, vol. 20, no. 5, pp. 1262-1275, May 2000.

[7] Y. Nakashima, T. N. Wight, and K. Sueishi, "Early atherosclerosis in humans: role of diffuse intimal thickening and extracellular matrix proteoglycans," Cardiovasc. Res., vol. 79, no. 1, pp. 14-23, Jul. 2008.

[8] L. Saba, R. Sanfilippo, R. Montisci, Jasjit S. Suri, S. Sannia, G. Mallarini, "Carotid artery wall thickness (CAWT) measured using Computed Tomography: Inter- and Intra-observer Agreement analysis," *AJNR Am. J. Neuroradiol.*, 2011.

[9] F. Molinari, G. Zeng, and J. S. Suri, "A state of the art review on intima-media thickness (IMT) measurement and wall segmentation techniques for carotid ultrasound," *Comp. Methods Programs Biomed.,* vol. 100, no. 3, pp. 201-221, Dec. 2010.

[10] F. Molinari, C. Pattichis, G. Zeng, L. Saba, R. U. Acharya, R. Sanfililippo, A. Nicolaides, and J. S. Suri, "Completely automated multi-resolution edge snapper (CAMES) - a new technique for an accurate carotid ultrasound IMT measurement: Clinical validation and benchmarking on a multi-institutional database," IEEE Trans Image Process 2011a (accepted; in-press).

[11] T. Ojala, M. Pietikäinen, and T. Maenpaa, "Multiresolution gray-scale and rotation invariant texture classification with local binary patterns," *IEEE Trans. Pattern Anal. Mach. Intell.*, vol. 24, no. 7, 971-987, Jul. 2002.

[12] K. I. Laws. Rapid texture identification. SPIE Conference Series, vol. 238, no. 376–380, 1980.

[13] M. Petrou and P. G. Sevilla, *Image Processing - Dealing with Texture*. John Wiley and Sons, 2006.

[14] I. M. Graf, F. H. Schreuder, J. M. Hameleers, W. H. Mess, R. S. Reneman, and A. P. Hoeks, "Wall irregularity rather than intima-media thickness is associated with nearby atherosclerosis," *Ultrasound Med. Biol.*, vol. 35, no. 6, pp. 955-961, Jun. 2009.

[15] J. Han, M. Kamber, and J. Pei, *Data Mining: Concepts and Techniques*. Morgan Kaufmann, 2005.

[16] J. F. Box, "Guinness, gosset, fisher, and small samples," *Statist. Sci.*, vol. 2, no. 1, pp. 45–52, 1987.

[17] E. C. Kyriacou, C. Pattichis, M. Pattichis, C. Loizou, C. Christodoulou, S. K. Kakkos, and A. Nicolaides, "A review of noninvasive ultrasound image processing methods in the analysis of carotid plaque morphology for the assessment of stroke risk," *IEEE Trans. Inf. Technol. Biomed.,* vol. 14, no. 4, pp. 1027–1038, Jul. 2010.

[18] S. G. Mougiakakou, S. Golemati, I. Gousias, A. Nicolaides, and K. Nikita, "Computer-aided diagnosis of carotid atherosclerosis based on ultrasound image statistics, laws' texture and neural networks," *Ultrasound Med. Biol.,* vol. 33, no. 1, pp. 26-36, Jan. 2007.

[19] E. Kyriacou, M. Pattichis, C. S. Pattichis, A. Mavrommatis, C. I. Christodoulou, S. Kakkos, and A. Nicolaides, "Classification of atherosclerotic carotid plaques using morphological analysis on ultrasound images," *J. Appl. Intell.,* vol. 30, no. 1, pp. 3–23, 2009.

[20] R. U. Acharya, O. Faust, A. P. Alvin, S. Vinitha Sree, F. Molinari, L. Saba, A. Nicolaides, and J. S. Suri, "Symptomatic vs. asymptomatic plaque classification in carotid ultrasound," *J. Med. Syst*., Jan 2011. DOI: 10.1007/s10916-010-9645-2.